



Published in final edited form as:

Mucosal Immunol. 2021 July ; 14(4): 887–898. doi:10.1038/s41385-021-00392-9.

Immune Modulation Mediated by Extracellular Vesicles of Intestinal Organoids is Disrupted by Opioids

Yue Zhang^{1,#}, Yan Yan^{1,#}, Jingjing Meng^{1,#}, Mohit Girotra², Sundaram Ramakrishnan¹, Sabita Roy^{1,*}

¹Department of Surgery, University of Miami, Miller School of Medicine, Miami, Florida 33101, USA

²Division of Gastroenterology, University of Miami, Miller School of Medicine

Abstract

Extracellular Vesicles (EVs) are effective mediators of intercellular communications between enterocytes and immune cells. The current study showed that EVs isolated from mouse and human intestinal organoids modulated inflammatory responses of various immune cells including mouse bone-marrow derived-macrophages, dendritic cells, microglia cells, and human monocytes. EVs suppressed LPS-elicited cytokine production in these cells while morphine abolished EVs' immune modulatory effects. Microarray analysis showed that various microRNAs, especially Let-7, contributed to EV-mediated immune modulation. Using murine models, we showed that injection of EVs derived from intestinal organoids reduced endotoxin-induced systemic inflammation and alleviated the symptoms of DSS-induced colitis. EVs derived from morphine-treated organoids failed to suppress the immune response in both these models. Our study suggests that EVs derived from intestinal crypt cells play crucial roles in maintaining host homeostasis and opioid use is a risk factor for exacerbating inflammation in patients with inflammatory diseases such as sepsis and colitis.

Introduction

The gastrointestinal tract is continuously exposed to food antigens and microbes. To maintain host homeostasis, the enterocytes have to communicate with the immune cells to keep the balances between tolerance to commensal bacteria and the ability to initiate efficient defense responses to harmful pathogens. The disturbance of intestinal homeostasis

Users may view, print, copy, and download text and data-mine the content in such documents, for the purposes of academic research, subject always to the full Conditions of use:http://www.nature.com/authors/editorial_policies/license.html#terms

*Correspondence to: Sabita Roy, Department of Surgery, University of Miami, Miller School of Medicine, Miami, Florida 33101, USA, sabita.roy@miami.edu, Phone: +1 (305) 2438452.

#Contribute equally.

Author Contributions

SR, YZ, YY and JM provided substantial contributions to the conception of the work. YZ, YY and JM initiated the study design and contribute equally in the acquisition, analysis or interpretation of data. MG and SR helped with the implementation of the study. All authors substantially contributed to the drafting, revising and critically reviewing the manuscript for important intellectual content.

Disclosure

The authors declare no competing financial interests.

Authors claim that there are no conflicts in interest.

results in autoimmune diseases such as inflammatory bowel disease (IBD), which is characterized by chronic and exacerbated inflammation in the gut.

Recently, it has been revealed that Extracellular Vesicles (EVs), the 30–100nm membranous vehicles, are able to mediate the interactions between intestinal epithelial cells and the immune system¹. EVs isolated from different tissue sources have been shown to generate multiple effects on the immune system. For instance, dendritic cell-derived EVs were shown to indirectly activate CD4 positive T cells², while intestinal epithelial cell-derived EVs play an important role in the induction of Treg cells³. Also, tumor-derived EVs have been shown to induce various immunomodulatory effects^{4,5}. Although the intestinal epithelial cells have been shown to be able to release EVs³, very few studies have been performed to understand whether the intestinal epithelium-derived EVs are able to modulate cytokine production in different types of immune cells and the physiological consequences of such modulation. In order to explore the role of EVs in inflammation, this study isolated EVs released by intestinal organoids and determined the inflammatory responses of different immune cells in the presence of these EVs. Intestinal organoid cultures are three-dimensional *in vitro* models that incorporate most of the physiologically relevant features of the *in vivo* intestinal tissue.

Our lab has previously reported that chronic morphine treatment could manipulate gut immune environment. More specifically, with regards to sepsis, this manipulation resulted in both persistent inflammation and higher mortality^{6,7}. To understand whether opioid treatment can interfere with the immune modulatory function of EVs, we characterized the effects of organoid-derived EVs on the responses of immune cells to endotoxin stimulation and investigated the role of morphine treatment in this process. To study whether the effects of EVs on immune cells were altered by morphine treatment, we utilized saline- or morphine- pre-treated mouse or human organoids as the donors of EVs and respective mouse bone-marrow derived-macrophages, dendritic cells, microglia cells, and human monocytes as the recipients.

We further identified the specific compositions of EVs secreted by saline- or morphine-treated organoids and demonstrated that multiple microRNAs especially Let7 were packaged in EVs. These microRNAs play crucial roles in maintaining normal immune function. Our results also suggested that Let7 delivered by EVs acted as a key molecular regulator controlling inflammation, which was compromised by use of opioids.

Results

Intestinal organoid-derived EVs inhibits endotoxin induced inflammatory cytokines in Bone marrow-derived dendritic cells (BMDC)

Initially we show that intestinal organoid maintained in conditioned medium with or without morphine (1 μ M) continuously secrete EVs. Multiple ultra-centrifugation⁸, or an ExoQuick Kit from System Biosciences was used to purify EVs from the supernatants of saline- or morphine-treated organoids. The EVs harvested from the supernatants were visualized using transmission electron microscopy (TEM). Our data show no significant difference in the shape and particle size distribution between two samples using different purification methods (Supplemental Figure1A), so we chose to use ExoQuick Kit for EV purification in

the following experiments. Western blot assays revealed that both samples contained high levels of the Exosome-specific protein markers CD63, CD9, and Tsg101, but have relatively low levels of β -actin compared to organoid cell lysate (Supplemental Figure 1B).

To determine if immune cells can take up exogenous EVs, we labeled organoid-secreted EVs with PKH67 dye (green) and incubated them with either a BMDC or BMM culture for 24 hours. Immunofluorescent images confirmed that recipient cells with F-actin (red) expression colocalized with PKH67-labeled EVs (Supplemental Fig. 2).

Next, to study the role of EVs in mediating immune responses in different cell types, we used the mouse intestinal organoid as an EV donor. When the recipient cells were BMDCs, our results showed that the treatment of EVs alone did not make any significant differences in the expression of pro-inflammatory cytokines. However, in the condition of LPS stimulation, EVs derived from saline-treated organoids (EV(Org/S)) significantly reduced the mRNA levels of pro-inflammatory cytokines like IL-6, TNF α and IL-1 β . In contrast, EVs derived from morphine-treated organoid (EV(Org/M)) did not significantly reduced the proinflammatory response (Figure 1A–C). In addition, EV(Org/S) increased LPS induced mRNA of anti-inflammatory cytokines IL-2, IL-10 and IL-25 (Figure 1D–F), while EV(Org/M) abolished this effect. The protein levels of IL-6 and TNF α were validated using ELISA (Figure 1G–H).

Under LPS stimulation condition, when BMDC were treated with the EVs that were derived from mouse colonic organoid, both IL-6 (Supplemental Figure 2A) and TNF α (Supplemental Figure 2B) protein levels were dramatically reduced in the supernatant. Cytokine reduction in the supernatant, however, was significantly negated by the EVs isolated from morphine-treated colonic organoid. Our results indicate that both small intestinal and colonic organoids are able to secrete EVs that can modulate cytokine expression in immune cells and this effect was negated by morphine treatment.

Bone marrow-derived macrophages (BMMs) and microglia exhibited similar responses to endotoxin stimulation after uptake of intestinal organoid-derived EVs.

When the recipient cells were BMMs, EVs' modulation of inflammatory response to LPS could be seen at both mRNA and protein levels (Figure 2). After LPS treatment, EV(Org/S) significantly reduced mRNA level of pro-inflammatory cytokines IL-6, TNF α and IL-1 β were observed, while these effects were abolished with EV(Org/M) from morphine treated organoids. (Figure 2A–C). Interestingly, EV(Org/S), but not EV(Org/M), increased mRNA levels of anti-inflammatory cytokines such as IL-2, IL-10 and IL-25 induced by LPS (Figure 2D–F). These effects were further validated using protein analysis. EV(Org/S) decreased the protein levels of IL-6 and TNF α in the supernatant of LPS activated BMM. Protein levels of these cytokines were not observed with EVs derived from morphine treated organoid (Figure 2G–H).

We next tested the impact of EV's on microglia as the recipient cells. Our results showed similar effects with that observed with BMM following LPS stimulation. EV(Org/S) significantly reduced the mRNA levels of pro-inflammatory cytokines TNF α , IL-6 and IL-1 β , while increasing the levels of anti-inflammatory cytokines IL-10. In contrast

EV(Org/M) significantly inhibited these effects (Supplementary Figure 3A–F). EV(Org/S) also decreased the IL-6 and TNF α protein levels in the supernatant of SIM-A9 microglial cells after LPS incubation, as shown by ELISA (Supplementary Figure 3G–H).

EVs derived from human colonic organoids modulated inflammatory cytokine expressions in differentiated THP-1 cells.

When we used human organoid culture as an EV donor and human macrophages as the recipient, we saw similar results as indicated above (Figure 3). EV(Org/S) could significantly reduce the mRNA levels of pro-inflammatory cytokines IL-6, TNF α , and IL-1 β in THP-1 cells after LPS stimulation, while EV(Org/M) did not have these effects (Figure 3A–C). EV(Org/S) also significantly decreased the secretion of IL-6 and TNF α proteins in supernatant of differentiated THP-1 after LPS incubation, while EV(Org/M) abolished these effects (Figure 3D–E).

Taken together, EVs derived from saline-treated organoids could suppress recipient cells' inflammatory responses to endotoxin stimulation. However, EVs derived from morphine-treated organoids did not have such effects. Next, we investigated the components of EVs in the presence and absence of morphine treatment.

MicroRNA profile in saline- or morphine-treated organoid derived-EVs show significant differences

It has been well established that microRNA could be delivered between cells by EVs, thus mediating cell-to-cell communication^{9–12}. We isolated the total RNA from EVs derived from saline- or morphine-treated organoid, and performed a real-time PCR based microRNA array assay. The results showed that although there were individual differences between samples within each group, some microRNAs, like miR23a, miR181a, and Let7c, still demonstrated significant differences in expression levels between EV(Org/S) and EV(Org/M), (Figure 4A). These microRNAs all have predicted target genes related to signaling pathways that were involved in inflammation (Figure 4B). For example, Let7c-5p potentially targets IL-6 and TLR4; IL-1 α is a predicted target of miR181a and miR410, while several microRNAs including miR302d would potentially regulate the expression of IL-25.

We then checked the levels of these individual microRNAs in the EVs that were derived from mouse small intestinal organoids treated with morphine. In the EVs from morphine-treated organoids, as shown in Figure 4C, Let7c-5p levels were decreased while the levels of miR186, miR181a, and miR302d were increased. These detected changes were consistent with the microRNA array results.

Next, we investigated if these microRNA level changes in EVs were correlated to the microRNA changes in the donor cells. Interestingly, the decrease in Let7c-5p, Let7b and miR23a levels and the increase in miR186 levels were also observed in the donor intestinal organoid (Figure 4D). These results indicated that the microRNA profile changes induced by morphine affected the microRNA packaging into the EVs. And the microRNA changes in the EVs interfered with the intercellular communication between the donor organoids and the recipient inflammatory cells.

We also determined the microRNA expression in human organoids and their EVs (Figure 4E and 4F). Interestingly, the dramatic decrease of Let7c-5p induced by morphine was consistently observed in mouse and human organoids and the EVs produced by these organoids.

As previously discussed, Let7c-5p has predicted targets of IL-6 and TLR4, with the former as an important cytokine in early immune response and the latter as the receptor specific for LPS. With our previous results demonstrating that, in the presence of EVs derived from intestinal organoids, IL-6 was decreased, we next tested whether the anti-inflammatory effects of EVs were mediated by Let7c-5p.

Effect of EVs on inflammatory cytokine expression was mediated by Let7c-5p

Let7c and other Let7 family microRNA have been shown to directly target IL-6 3'UTR (Figure 5A) and downregulate IL-6 expression levels^{13,14}. Here we transfected an LNA-enhanced antisense miRNA inhibitor into BMDC, which efficiently reduced the Let7c-5p levels and inhibited the microRNA's function (Figure 5B). As shown in Figure 5C, when the negative control (NC) inhibitor was transfected into BMDC and the transfected BMDC were treated with LPS to simulate inflammatory response, the IL-6 mRNA expression was dramatically induced. And the IL-6 mRNA level was decreased with the treatment of EVs derived from mouse small intestinal organoid. However, when the Let7c-5p inhibitor was present in BMDC cells, the EVs could no longer reduce IL-6 mRNA levels (Figure 5C). The IL-6 protein levels showed the same trend (Figure 5D). These results suggested that when Let7c-5p was delivered into BMDC by EVs, it could directly target IL-6 and inhibit IL-6 expression. Additionally, the EV induced changes of TNF α mRNA (Figure 5E) and protein level (Figure 5F) were also influenced by the Let7c inhibitor in BMDC, but not as much as IL-6. This study demonstrated that Let7c-5p plays an important role in the anti-inflammatory effect of organoid EVs on recipient BMDC cells.

EVs exhibited anti-inflammatory effects in LPS-induced sepsis model

After we confirmed that EVs derived from saline-treated intestinal organoids could suppress immune responses stimulated by LPS *in vitro*, we investigated whether this effect could also be seen *in vivo*. An LPS-induced acute inflammation mouse model (Figure 6A) was used to measure the pro-inflammatory cytokines in plasma and spleen. The results showed that intravenous injection of saline-treated intestinal organoid-derived EVs could significantly reduce IL-6 (Figure 6B) and TNF α (Figure 6C) protein levels in the plasma, but not in the spleen (Figure 6D–E). Injection of morphine-treated intestinal organoid-derived EVs, however, abolished this effect. These data further support our conclusion that EVs derived from saline-treated intestinal organoid have an anti-inflammatory effect on the immune system.

EVs treatment resulted in decreased severity in a DSS-colitis model

To further investigate whether EVs also modulate local intestinal inflammation, the DSS induced colitis model in C57BL/6 mice (Figure 7A) was used. By adding DSS in the drinking water for 9 days, mice exhibited dramatic weight loss and shortening of the colons (Figure 7 B–D). Using the weight loss (Figure 7B) and shortening of the colons (Figure 7 C–

D) as indicators of the severity of colitis, we observed that intravenous injection of saline-treated intestinal organoid-derived EVs prior to DSS-inducement (ES+DSS) could significantly alleviate the severity of colitis. On the other hand, morphine-treated intestinal organoid-derived EVs (EM+DSS) abolished these effects. Representative H&E-stained sections showed that DSS caused extensive inflammation induced damage on the colon tissue, when compared to both DSS and EM+DSS groups, organoid-derived EVs could ameliorate the extent of the damage (Figure 7E–F). EVs also inhibited the induction of serum inflammation in DSS-treated mice, as shown by IL-6 ELISA (Figure 7G). Yet the expression of TNF α was not affected by EV injection. Taken together, these data support our conclusion that saline-treated intestinal organoid-derived EVs have a protective effect on the DSS-induced colitis, by reducing excessive inflammation induced damage in the colon.

Let7c-5p levels in EVs isolated from plasma, small intestine, and large intestine were reduced in DSS/Morphine treated mice

Our earlier study has shown that morphine could exaggerate DSS-induced **mucosal inflammation** syndrome¹⁵. As shown in Figure 7, the EVs that are derived from intestinal organoid, rather than morphine-treated organoid, could efficiently alleviate colitis. In addition, Let7c-5p was suggested to be an important component in the EVs that mediated the anti-inflammatory effect (Figure 5). We initially investigated if Let7c-5p levels in the EVs were altered when the mice underwent DSS-induced **mucosal inflammation** syndrome. When DSS was added to the drinking water for 9 days (Figure 8A), the body weight of the mice was decreased (Figure 8B) and their colon lengths were reduced (Figure 8C). When the mice were injected with Morphine at the same time, the effects were more dramatic with greater weight loss and more severe colon length shortening (Figure 8B and 8C). We isolated the EVs from the plasma, small intestinal tissue as well as large intestinal tissue, and measured the Let7c-5p levels in the EVs. In the DSS-treated mice, Let7c-5p in both the plasma EVs (Figure 8D) and small intestine EVs (Figure 8E) were dramatically reduced. In addition, when the mice were treated with Morphine, Let7c-5p levels was significantly and further reduced in EVs derived from both small intestine (Figure 8E) and large intestine (Figure 8F).

These findings were consistent with our *in vitro* data (Figure 4) showing the morphine treatment would reduce the Let7c-5p levels in both intestinal organoid and its secreted EVs. Since Let7c levels were already dramatically reduced by DSS, the combination of morphine and DSS didn't show a synergistic effect. Interestingly, when mice were treated with DSS, neither Let7c nor the U6 microRNAs was detected in the large intestine. It is plausible that the dramatic decrease in EV secretion may be a consequence of significant cellular damage caused by DSS treatment. These studies suggest that the reduced Let7c-5p in the circulating EVs or within the local intestinal environment contribute to DSS triggered-inflammation in the gut. This effect can be further exacerbated by morphine treatment by reducing Let7c-5p levels in the intestine.

Discussion

In this study, we demonstrate that the extracellular vehicles (EVs) secreted by crypt cells derived from small and large intestines play an important role in maintaining the intestinal mucosal homeostasis. We provide evidence that specific miRNAs transported by these EVs are used by the immune system to fine-tune immune responses to various exogenous stimulations.

Our results also indicate that EV-mediated immune modulation can be significantly influenced by various factors like opioid exposure. Opioids are commonly prescribed for pain management in patients who are suffering from acute or chronic pain. For example, a population-based analysis indicates that the likelihood of being exposed to an opioid following a diagnosis of IBD was 72 % at 10 years post-diagnosis¹⁶. Due to their analgesic and sedative activities, opioids are frequently used to treat hospitalized patients¹⁷. Multiple clinical studies show that opioid use is associated with worse outcomes of inflammatory diseases including IBD and sepsis^{18–20}. However, the mechanistic role of opioid in disease progression still remains poorly understood. Numerous animal studies suggest that opioid treatment can disrupt the tightly balanced tolerance to inflammation, resulting in abnormal inflammatory responses, accelerated disease progression, and poor prognosis. Using the murine model of DSS-induced colitis and spontaneous colitis (IL-10 knock out mice), we recently showed that hydromorphone exacerbated colitis. Hydromorphone treatment enhanced proinflammatory cytokine production and subsequent intestinal tissue damage in both mouse models of **mucosal inflammation**, which was consistent with morphine's effects observed in the present study¹⁵. Furthermore, we previously showed in two sepsis models, one of which was sepsis induced by LPS and the other was sepsis induced by Cecal-ligation puncture, morphine caused persistent or excessive inflammatory responses^{6,7}. However, the mechanisms underlying how opioid use disrupts host immune homeostasis is still not clear.

In this study, we provide evidence that opioid treatment can disrupt gut immune homeostasis by inhibiting packaging of miRNA into EVs secreted by intestinal crypt cells. We also identified Let7 as the crucial microRNA in EVs that was able to modulate inflammatory responses of various immune cells. Morphine treatment led to a decrease in EV's Let7 levels, resulting in abnormal inflammatory responses of bystander immune cells in the intestine.

Our findings indicate the possible therapeutic implications of EV loaded microRNAs. In physical conditions, EVs secreted by the intestinal crypt cells seems to have a beneficial effect on the LPS-induced sepsis mice and DSS-induced inflammation mice models. For example, Ma et al found that the exosomes released from mesenchymal stromal cells is reported to possess an immunosuppressive effect *in vitro* and exhibit a therapeutic capability in a mouse model of DSS-induced colitis²¹. In another study, the exosomes derived from granulocytic myeloid-derived suppressor cells were shown to attenuate DSS-induced colitis through inhibiting Th1 cells proliferation and promoting Tregs expansion²². However, the exact contents transferred by EVs that were able to shape the immune system that reside within the intestinal mucosa has not been characterized in these studies.

EVs contain proteins, lipids as well as nucleic acids such as DNA, mRNA, and non-coding RNAs²³. EV-mediated transfer of microRNAs has been shown to be an important mechanism of genetic exchange between cells¹. EVs carrying the microRNAs, such as miR181, miR155, and Let7, function as immune modulators²⁴. Alexander et al, showed that exosome-delivered microRNAs, including miR155 and miR146a, differentially modulate the inflammatory response to endotoxin¹⁰. Here, we detected almost one hundred microRNAs in the EVs that were derived from small intestinal organoids (Figure 4A). In addition, we found that microRNA levels in both the EVs and the donor organoids were changed by morphine treatment (Figure 4B, 4C, 4D), indicating that morphine might exert its gut immune-regulatory effect, at least partially, through modulating the microRNA expression levels in the intestinal crypts. As a result, morphine may impact the cargo of secreted EVs which would transfer these regulatory microRNA molecules to the recipient immune cells. One of these important microRNAs is Let7c-5p. Let7c and other Let7 family microRNA have been shown to directly target IL-6 3'UTR and downregulate IL-6 expression which is involved in inflammatory response^{13,14}. Our study showed that the Let7c-5p levels in the morphine-treated organoid EVs was significantly reduced, and these EVs could no longer inhibit the IL-6 expression in the recipient BMDC. In addition, the presence of the Let7c-5p inhibitor in these BMDC efficiently abolished the anti-inflammatory effect of the naïve organoid EVs (Figure 5). These results suggest the important role of EVs that contain Let7c-5p in the communication between the gut crypt and the local/distal immune cells. However, we cannot completely exclude the potential roles of other miRNAs in the EVs, such as miR186 and miR23a, both of which also target cytokines or inflammatory molecules (Figure 4B). Future functional studies regarding these microRNAs or other nucleic acid molecules and proteins in the EVs will give us deeper insight of the EV-mediated intracellular communication, and more importantly will unravel some novel EV-based therapeutic strategy.

The prevalence of EVs in body fluid including plasma, urine, saliva and gut mucus not only supports the hypothesis that EVs exert important functions in physiological and pathological processes, but also suggests their potential roles as biomarkers, especially under pathological conditions²⁴. EV-microRNAs have been tested as biomarkers for cancer diagnosis and prognosis. An elevated serum exosomal miR-21 level was observed in pancreatic adenocarcinoma, while miR17-5p was shown to correlate with cancer stages²⁵ and a subset of serum exosomal microRNAs was shown to be an early biomarker for AML²⁶. In our study of DSS-induced mucosal inflammation mouse model, Let7c-5p levels in the plasma EVs were dramatically decreased (Figure 8D) when the mice were treated with DSS and exhibited enhanced inflammation in the gut. This result further supported our earlier hypothesis that the intestinal EVs inhibited inflammatory response through Let7c-5p under normal conditions; DSS or morphine treatment, however, decreased the amount of Let7c-5p in the plasma or intestinal EVs, resulting in pathogenic inflammation in the gut. These observations suggested that the level of Let7c-5p in the plasma EVs could be applied as a potential clinical biomarker for IBD due to its ease of access and stability.

Our current study suggests the potential role of intestinal EVs in maintaining the gut immune homeostasis by secreting microRNAs that modulate the inflammatory responses of bystander immune cells. Morphine treatment results in the change of components in the

EVs, especially the decrease of Let7, eventually disrupting the homeostasis in the gut and causing more severe inflammation. Our study provides new evidence to support the application of EVs as either a diagnostic tool or a therapeutic approach for controlling inflammatory diseases, such as sepsis and colitis. In addition, our findings also demonstrate the implications of EVs, like exosomes, as useful vectors for mediating microRNA delivery in the development of novel therapeutic strategies.

Methods

Animals

Eight-week-old C57BL/6J (WT) mice were purchased from Jackson Laboratories (Bar Harbor, ME, USA) (<https://www.jax.org/strain/003752>). Animal maintenance and procedures were conducted according to the Institutional Animal Care and Use Committee (IAUCUC) policies at the University of Miami.

Mice received intravenous injections of 1mg (total protein) organoid-derived EVs in PBS. Twenty-four hours later, mice received 500ng/kg lipopolysaccharide (LPS) by intraperitoneal (i.p.) injection. Two hours later, mice were sacrificed and their serum, spleen were processed for cytokine measurement by ELISA. For colitis model, four groups of mice received tail-vein injection of PBS or EVs on day 0, and then three experimental groups of mice received 2.5% dextran sulfate sodium (DSS) in drinking water for 9 days while control group received normal water. The body weight of each group of animals was recorded every two days. On day 10, mice were sacrificed, and intestinal damage was accessed by histological analysis.

Cell Culture

C57BL/6J mice were sacrificed and their femur bones were removed for bone-marrow primary culture. Bone-marrow cells were maintained in complete Iscove modified Dulbecco medium (IMDM; Gibco, Gaithersburg, MD, US), supplemented with 10% fetal bovine serum (FBS), 1% Penicillin/Streptomycin. Bone marrow-derived Dendritic Cells (BMDCs) were generated by 10 to 12 days of differentiation in complete medium added with 20ng/ml granulocyte macrophage-colony stimulating factor (GM-CSF), and 10ng/ml recombinant mouse IL-4 protein (R&D Systems, MN, US). Bone marrow-derived Macrophages (BMMs) were generated by 6 to 7 days of differentiation in complete medium added with 20ng/ml mouse macrophage-colony stimulating factor (M-CSF). Fluorescence activated cell-sorting (FACS) analysis were used to validate these cell types.

The SIM-A9 mouse microglia cell line were purchased from ATCC (<https://www.atcc.org/products/all/CRL-3265>) and maintained in DMEM:F12 Medium (Gibco, Gaithersburg, MD, US), supplemented with 5% heat-inactivated horse serum, 10% fetal bovine serum (FBS) and 1% Penicillin/Streptomycin.

The THP-1 human monocyte cell line were purchased from ATCC (<https://www.atcc.org/products/all/TIB-202>) and maintained in RPMI-1640 Medium (Gibco, Gaithersburg, MD, US), supplemented with 0.05 mM 2-mercaptoethanol, 10% fetal bovine serum (FBS) and

1% Penicillin/Streptomycin. These monocytes were differentiated into macrophages by 24 h incubation with 150 nM phorbol 12-myristate 13-acetate (PMA, Sigma, P8139)

Organoid Culture

Intestinal organoid cultures were established using the intestinal crypts isolated from the mouse or human samples as previously described^{27,28}. For mouse intestinal organoid culture, the intestines were opened longitudinally and washed with cold phosphate-buffered saline (PBS). The tissue was then cut into 2 to 4 mm pieces and further washed at least 10 times by pipetting up and down with cold PBS. Tissue fragments were incubated with Gentle Cell Dissociation Reagent (STEMCELL Technologies) for 15 min at room temperature. After removal of the Cell Dissociation Reagent, tissue fragments were washed with PBS to release crypts. Supernatant fractions enriched in crypts were collected, passed through a 70 µm cell strainer, and centrifuged at 300 g for 5 min. The cell pellet was resuspended with Dulbecco's modified Eagle medium/F12 medium and centrifuged at 200 g. Crypts were then entrapped in Matrigel (growth factor reduced; BD Bioscience) and cultured using advanced Dulbecco's modified Eagle medium/F12 containing various growth factors in the presence or absence of 1 µM morphine. Human colon samples were obtained from patients undergoing colonoscopy at University of Miami Hospital with written informed consent under an approval of the ethical committee (IRB Number 20160338). Non-inflamed colon samples from two patients were used in this study. Collected tissues were transferred into cold PBS and placed on ice until use. Colon tissues were minced into small pieces. Tissue fragments were processed and cultured using the same protocol as for the mouse organoid culture. The human organoids were grown in conditioned medium produced by a supportive L-WRN cell line as previously described²⁹.

Isolation of EVs from culture medium, mouse plasma, small intestine and large intestine

Extracellular Vesicles (EVs) were recovered from the supernatant of cultured organoids for 72 hours. The supernatants were centrifuged at 3000g for 10 min to remove cell debris, then purified by filtration on 0.22 µm pore filters, followed by ultracentrifugation at 100 000g at 4°C for 2.5 hours as described before, or using an ExoQuick isolation kit (System Biosciences, Palo Alto, CA, US) based on the manufacturer's protocol. In each EV preparation, the concentration of total proteins was quantified by Bradford assay (Bio-Rad, Hercules, CA, US). The size and shape of Extracellular Vesicles were visualized with Transmission Electron Microscopy (TEM) in the University of Miami TEM imaging core as described.

EVs were collected from the plasma using the ExoQuick Plasma Prep with Thrombin kit (System Biosciences, Palo Alto, CA, US) according to the manufacturer's protocol. Briefly, plasma samples (~200µl) were pretreated with thrombin. After centrifugation at 10,000rpm for 5mins, the supernatant was transferred to a fresh tube and treated with ExoQuick precipitation reagent to precipitate the exosome which was lysed directly with Qiazol reagent (miRNeasy Mini Kit, Qiagen) for microRNA extraction.

Intestinal tissues were detached (~5cm), cut into small pieces and enzymatically digested for 2Hrs with 1mg/ml type II collagenase (STEMCELL technology, Cat# 07418) as described

before³⁰. The tissue fragments were centrifuged at 300g for 10min, after which the supernatant was collected and filtered through the 0.22µm filter. Exosome was isolated from the filtered solution using the ExoQuick isolation kit (System Biosciences, Palo Alto, CA, US) according to the manufacturer's protocol. Exosome was then lysed directly with Qiazol reagent (miRNeasy Mini Kit, Qiagen) for microRNA extraction.

Western Blot

Total proteins (20 µg) were extracted from intestinal organoids or EV pellets lysed with radio-immunoprecipitation assay (RIPA) buffer (Thermo Fisher Scientific, Waltham, MA, US) plus fresh protease and phosphatase inhibitors (Roche, Indianapolis, IN, US), then loaded to each lane and separated by sodium dodecyl sulfate polyacrylamide gel electrophoresis, and then transferred to a 0.45 µm pore size nitrocellulose membrane (Bio-Rad, Hercules, CA, US). The antibodies used in western blot assay were shown in table 1.

Immunocytochemistry

To determine whether recipient cells have the ability to take up EVs, a lipid-associating fluorescent dye (PKH67; Sigma- Aldrich, St. Louis, MO, US) was used to label EVs as previously described. BMDCs were grown in the Nunc™ Lab-Tek™ II Chamber Slide™ (Thermo Fisher Scientific, Waltham, MA, US). Fluorescent-labeled EVs or PBS-PKH67 controls were washed by PBS and IMDM medium, then incubated with cells for 24 h. On the next day, cells were washed twice with PBS, fixed with with 4% paraformaldehyde, and were stained with F actin antibody (Thermo Fisher Scientific, Waltham, MA, US) for 60 min. Sample slides were washed with PBS and mounted with DAPI anti-fade reagent. Images were obtained using a Leica Microscope.

Histological Evaluation

Hematoxylin and eosin (H&E) staining was performed by Pathology Research Resources Laboratory at University of Miami. The pathological score was evaluated using histological scoring system as previously described³¹.

Quantitative real-time PCR

Total RNAs were isolated from EVs or organoids with TRIzol reagent (Invitrogen Life Technologies, Carlsbad, CA, US). The levels of multiple cytokines were detected by quantitative real-time PCR using the High Capacity cDNA Reverse Transcription Kit (Thermo Fisher Scientific, Waltham, MA, US) and the LightCycler® 480 System (Roche, Indianapolis, IN, US). Primers used for Quantative rt-PCR were shown in table 2.

MicroRNA PCR Arrays

The detection and quantification of microRNA from cells, EVs, or organoids were performed with miScript PCR System (Qiagen, Hilden, Germany). Briefly, cDNA is prepared using the miScript II RT Kit with total RNA isolated from cells, EVs or organoids and is used as template in real-time PCR with the miScript miRNA PCR Array and SYBR Green PCR Kit. **Data analysis is based on the CT method with normalization of the**

raw data to the housekeeping genes including: SNORD61, SNORD68, SNORD72, SNORD95, SNORD96A and RNU6–6P.

The miScript Primer Assays of designed primers combined with an endogenous reference RNA (U6) were used to evaluate the variability of expression level of target microRNAs in EVs derived from saline or morphine-treated organoids.

Transfection of LNA microRNA inhibitor

LNA-enhanced antisense microRNA negative control inhibitor or Let7c-5p inhibitor (Qiagen) was added directly into the culture medium of BMDC at the concentration of 100nM. 72Hrs later, the cells were collected to check the Let7c-5p level or treated with organoid-derived EVs and LPS.

Enzyme-linked immunosorbent assay (ELISA)

EVs were added to recipient cells, cultured in Bovine Exosome-free medium in 6-well plates for 24 h. Conditioned medium was collected and centrifuged (3000 g) to clear the supernatants, which were subsequently used for cytokine detection by ELISA. For in vivo experiments, serum and spleen from mice were processed for cytokine detection. Cytokines in the cell culture supernatant or animal organs were detected by TNF- α and IL-6 ELISA kits (Invitrogen Life Technologies, Carlsbad, CA, US) according to the manufacturer's protocols. The Cytokine concentrations were determined by absorbance in triplicates with a Spectra Max M5 plate reader, running Softmax Pro 5 software.

Statistics

Data were presented as mean \pm SEM. Statistical analysis was performed with GraphPad Prism 6.0 (GraphPad Software, San Diego, CA) software. Unpaired Student t-test or one-way analysis of variance was adopted for analysis. Significance levels were denoted as *p < 0.05, **p < 0.01, or ***p < 0.001.

Supplementary Material

Refer to Web version on PubMed Central for supplementary material.

Acknowledgments

This work received support from the National Institutes of Health grants R01 DA050542, R01 DA043252, R01 DA037843, R01 DA044582, R01 DA047089, and R01DA050542 and Florida state grant, William G. "Bill" Bankhead, Jr., and David Coley Cancer Research Program 20B12 to SR, and from the Miami Center for AIDS research (CFAR) at the University of Miami Miller School of Medicine funded by a grant P30AI073961 from the National Institutes of Health (NIH) to JM. We thank Dr. Maria Abreau for providing us L-WRN cell line and human organoid culture.

References:

1. Valadi H, Ekström K, Bossios A, Sjöstrand M, Lee JJ, Lötvall JO. Exosome-mediated transfer of mRNAs and microRNAs is a novel mechanism of genetic exchange between cells. *Nat Cell Biol.* 2007;9(6):654–659. doi:10.1038/ncb1596 [PubMed: 17486113]

2. Théry C, Duban L, Segura E, Véron P, Lantz O, Amigorena S. Indirect activation of naïve CD4 + T cells by dendritic cell – derived exosomes. *Nat Immunol.* 2002;3(12):1156–1162. doi:10.1038/ni854 [PubMed: 12426563]
3. Li T-L, Song C-H, Chen X-M, et al. Intestinal epithelial cell-derived integrin $\alpha\beta 6$ plays an important role in the induction of regulatory T cells and inhibits an antigen-specific Th2 response. *J Leukoc Biol.* 2011;90(4):751–759. doi:10.1189/jlb.1210696 [PubMed: 21724807]
4. Valenti R, Huber V, Iero M, Filipazzi P, Parmiani G, Rivoltini L. Tumor-released microvesicles as vehicles of immunosuppression. *Cancer Res.* 2007;67(7):2912–2915. doi:10.1158/0008-5472.CAN-07-0520 [PubMed: 17409393]
5. Bretz NP, Ridinger J, Rupp AK, et al. Body fluid exosomes promote secretion of inflammatory cytokines in monocytic cells via Toll-Like receptor signaling. *J Biol Chem.* 2013;288(51):36691–36702. doi:10.1074/jbc.M113.512806 [PubMed: 24225954]
6. Banerjee S, Meng J, Das S, et al. Morphine induced exacerbation of sepsis is mediated by tempering endotoxin tolerance through modulation of miR-146a. *Sci Rep.* 2013;1:1–12. doi:10.1038/srep01977
7. Meng J, Banerjee S, Li D, et al. Opioid Exacerbation of Gram-positive sepsis, induced by Gut Microbial Modulation, is Rescued by IL-17A Neutralization. *Sci Rep.* 2015;5(January):10918. doi:10.1038/srep10918 [PubMed: 26039416]
8. Théry C, Clayton A, Amigorena S, Raposo and G. Isolation and Characterization of Exosomes from Cell Culture Supernatants. *Curr Protoc Cell Biol.* 2006.
9. Baer C, Lyle R, Burdet F, et al. Endogenous RNAs Modulate MicroRNA Sorting to Exosomes and Transfer to Acceptor Cells. *Cell Rep.* 2014;8(5):1432–1446. doi:10.1016/j.celrep.2014.07.035 [PubMed: 25159140]
10. Alexander M, Hu R, Runtsch MC, et al. Exosome-delivered microRNAs modulate the inflammatory response to endotoxin. *Nat Commun.* 2015;6:7321. doi:10.1038/ncomms8321 [PubMed: 26084661]
11. Mittelbrunn M, Gutiérrez-Vázquez C, Villarroya-Beltri C, et al. Unidirectional transfer of microRNA-loaded exosomes from T cells to antigen-presenting cells. *Nat Commun.* 2011;2(1). doi:10.1038/ncomms1285
12. Xu AT, Lu JT, Ran ZH, Zheng Q. Exosome in Intestinal Mucosal Immunity. *J Gastroenterol Hepatol.* 2016;31:1694–1699. doi:10.1111/jgh.13413 [PubMed: 27061439]
13. Iliopoulos D, Hirsch HA, Struhl K. An Epigenetic Switch Involving NF- κ B, Lin28, Let-7 MicroRNA, and IL6 Links Inflammation to Cell Transformation. *Cell.* 2009;139(4):693–706. doi:10.1016/j.cell.2009.10.014 [PubMed: 19878981]
14. Sung SY, Liao CH, Wu HP, et al. Loss of let-7 microRNA upregulates IL-6 in bone marrow-derived mesenchymal stem cells triggering a reactive stromal response to prostate cancer. *PLoS One.* 2013;8(8). doi:10.1371/journal.pone.0071637
15. Sharma U, Olson RK, Erhart FN, et al. Prescription Opioids induce Gut Dysbiosis and Exacerbate Colitis in a Murine Model of Inflammatory Bowel Disease. *J Crohn’s Colitis.* 2019:1–17. doi:10.1093/ecco-jcc/jjz188 [PubMed: 30272119]
16. Targownik LE, Nugent Z, Singh H, Bugden S, Bernstein CN. The prevalence and predictors of opioid use in inflammatory bowel disease: a population-based analysis. *Am J Gastroenterol.* 2014;109(10):1613–1620. doi:10.1038/ajg.2014.230 [PubMed: 25178702]
17. Devlin JW, Roberts RJ. Pharmacology of Commonly Used Analgesics and Sedatives in the ICU: Benzodiazepines, Propofol, and Opioids. *Crit Care Clin.* 2009;25(3):431–449. doi:10.1016/j.ccc.2009.03.003 [PubMed: 19576523]
18. Burr NE, Smith C, West R, Hull MA, Subramanian V. Increasing Prescription of Opiates and Mortality in Patients With Inflammatory Bowel Diseases in England. *Clin Gastroenterol Hepatol.* 2018;16(4):534–541.e6. doi:10.1016/j.cgh.2017.10.022 [PubMed: 29079223]
19. Cross RK, Wilson KT, Binion DG. Narcotic use in patients with Crohn’s disease. *Am J Gastroenterol.* 2005;100(10):2225–2229. doi:10.1111/j.1572-0241.2005.00256.x [PubMed: 16181373]

20. Zhang R, Meng J, Lian Q, et al. Prescription opioids are associated with higher mortality in patients diagnosed with sepsis : A retrospective cohort study using electronic health records. *PLoS One*. 2018;1–8.
21. Ma ZJ, Wang YH, Li ZG, et al. Immunosuppressive effect of exosomes from mesenchymal stromal cells in defined medium on experimental colitis. *Int J Stem Cells*. 2019;12(3):440–448. doi:10.15283/ijsc18139 [PubMed: 31242720]
22. Wang Y, Tian J, Tang X, et al. Exosomes released by granulocytic myeloid-derived suppressor cells attenuate DSS-induced colitis in mice. *Oncotarget*. 2016;7(13):15356–15368. doi:10.18632/oncotarget.7324 [PubMed: 26885611]
23. Raposo G, Stoorvogel W. Extracellular vesicles: Exosomes, microvesicles, and friends. *J Cell Biol*. 2013;200(4):373–383. doi:10.1083/jcb.201211138 [PubMed: 23420871]
24. Corrado C, Raimondo S, Chiesi A, Ciccica F, De Leo G, Alessandro R. Exosomes as intercellular signaling organelles involved in health and disease: Basic science and clinical applications. *Int J Mol Sci*. 2013;14(3):5338–5366. doi:10.3390/ijms14035338 [PubMed: 23466882]
25. Que R, Ding G, Chen J, Cao L. Analysis of serum exosomal microRNAs and clinicopathologic features of patients with pancreatic adenocarcinoma. *World J Surg Oncol*. 2013;11(1):1. doi:10.1186/1477-7819-11-219 [PubMed: 23281640]
26. Hornick NI, Huan J, Doron B, et al. Serum Exosome MicroRNA as a minimally-invasive early biomarker of AML. *Sci Rep*. 2015;5:1–12. doi:10.1038/srep11295
27. Yin X, Farin HF, Van Es JH, Clevers H, Langer R, Karp JM. Niche-independent high-purity cultures of Lgr5 + intestinal stem cells and their progeny. *Nat Methods*. 2014;11(1):106–112. doi:10.1038/nmeth.2737 [PubMed: 24292484]
28. Sato T, Stange DE, Ferrante M, et al. Long-term expansion of epithelial organoids from human colon, adenoma, adenocarcinoma, and Barrett’s epithelium. *Gastroenterology*. 2011;141(5):1762–1772. doi:10.1053/j.gastro.2011.07.050 [PubMed: 21889923]
29. Miyoshi H, Stappenbeck TS. In vitro expansion and genetic modification of gastrointestinal stem cells in spheroid culture. *Nat Protoc*. 2013;8(12):2471–2482. doi:10.1038/nprot.2013.153 [PubMed: 24232249]
30. Jiang L, Shen Y, Guo D, et al. EpCAM-dependent extracellular vesicles from intestinal epithelial cells maintain intestinal tract immune balance. *Nat Commun*. 2016;7:1–15. doi:10.1038/ncomms13045
31. Engel MA, Kellermann CA, Rau T, Burnat G, Hahn EG, Konturek PC. Ulcerative colitis in AKR mice is attenuated by intraperitoneally administered anandamide. *J Physiol Pharmacol*. 2008;59(4):673–689. [PubMed: 19212003]

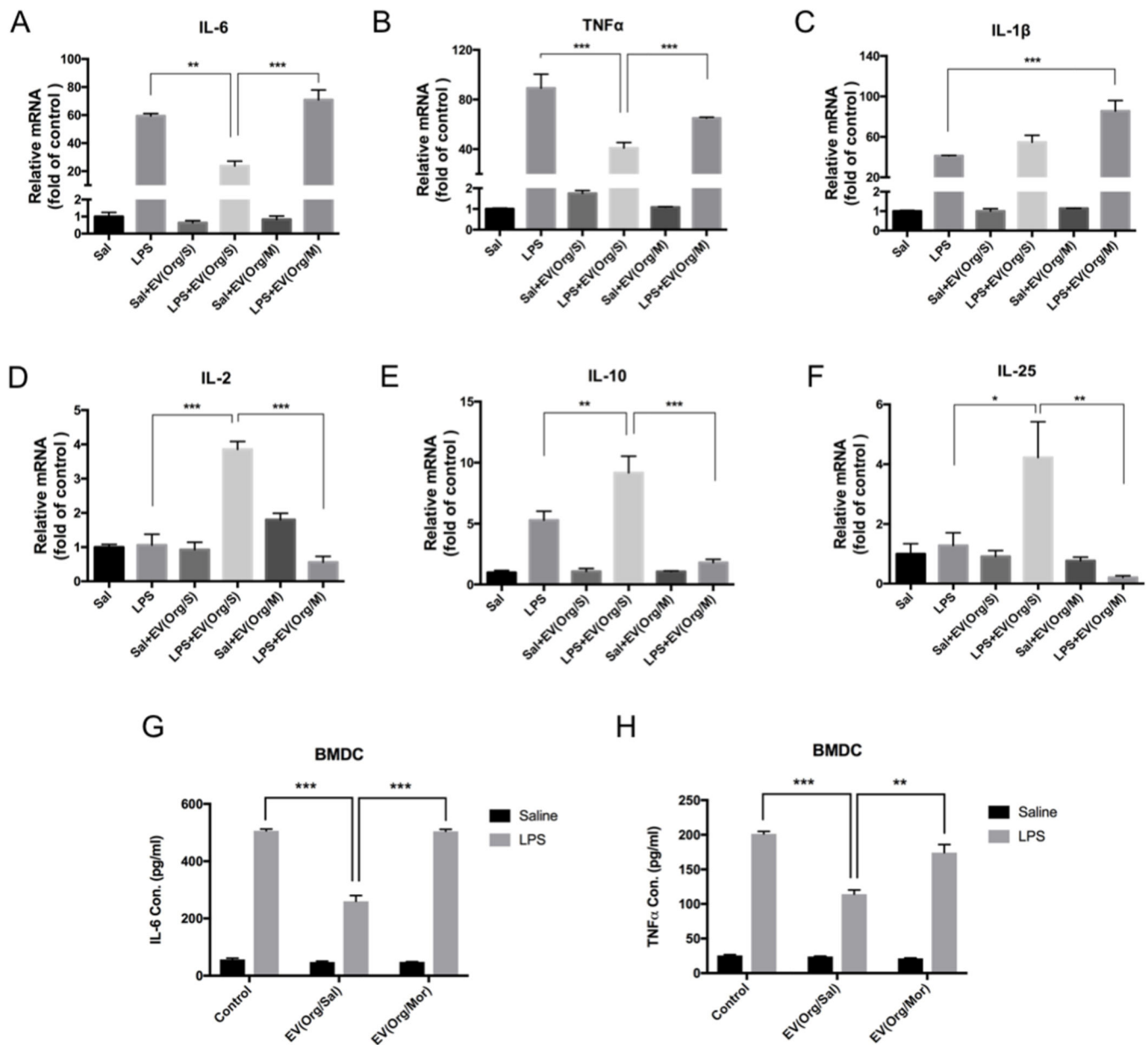


Figure 1. EVs modulated immune responses of mouse BMDC to endotoxin stimulation. The BMDC were incubated with saline-treated organoid-derived EVs (EV(Org/S)) or morphine-treated organoid-derived EVs (EV(Org/M)) and then stimulated with LPS for 4 hours. Total RNA of BMDC were purified for qPCR and the supernatant of BMDC was collected for ELISA. qPCR analysis of the IL-6 (A), TNF α (B), IL-1 β (C), IL-2 (D), IL-10 (E), and IL-25 (F). ELISA analysis of IL-6 (G) and TNF α (H). (sal: saline; LPS: Lipopolysaccharide; EV(Org/S): Extracellular Vesicles purified from the supernatant of organoid culture pretreated with saline; EV(Org/M): Extracellular Vesicles purified from the supernatant of organoid culture pretreated with morphine. The results are expressed as the mean \pm SEM of triplicate measurements in each group, * p <0.05, ** p <0.01, *** p <0.001).

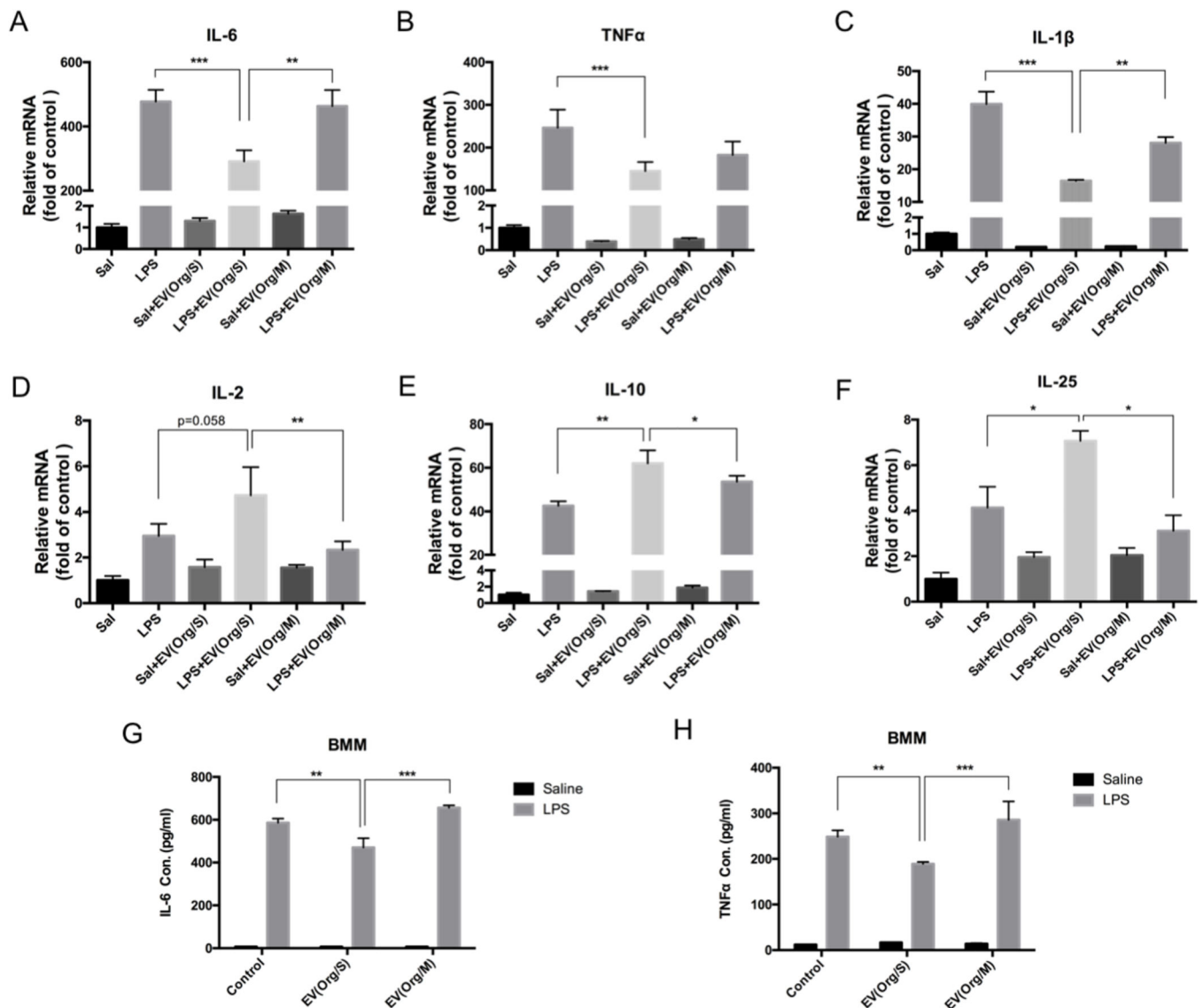


Figure 2. EVs modulated immune responses of mouse BMM to endotoxin stimulation. The BMM were incubated with saline-treated organoid-derived EVs (EV(Org/S)) or morphine-treated organoid-derived EVs (EV(Org/M)) and then stimulated with LPS for 4 hours. Total RNA of BMM were purified for qPCR and the supernatant of BMM was collected for ELISA. qPCR analysis of the IL-6 (A), TNF α (B), IL-1 β (C), IL-2 (D), IL-10 (E), and IL-25 (F). ELISA analysis of IL-6 (G) and TNF α (H). (sal: saline; LPS: Lipopolysaccharide; EV(Org/S): EVs purified from the supernatant of organoid culture pretreated with saline; EV(Org/M): EVs purified from the supernatant of organoid culture pretreated with morphine. The results are expressed as the mean \pm SEM of triplicate measurements in each group, * p <0.05, ** p <0.01, *** p <0.001).

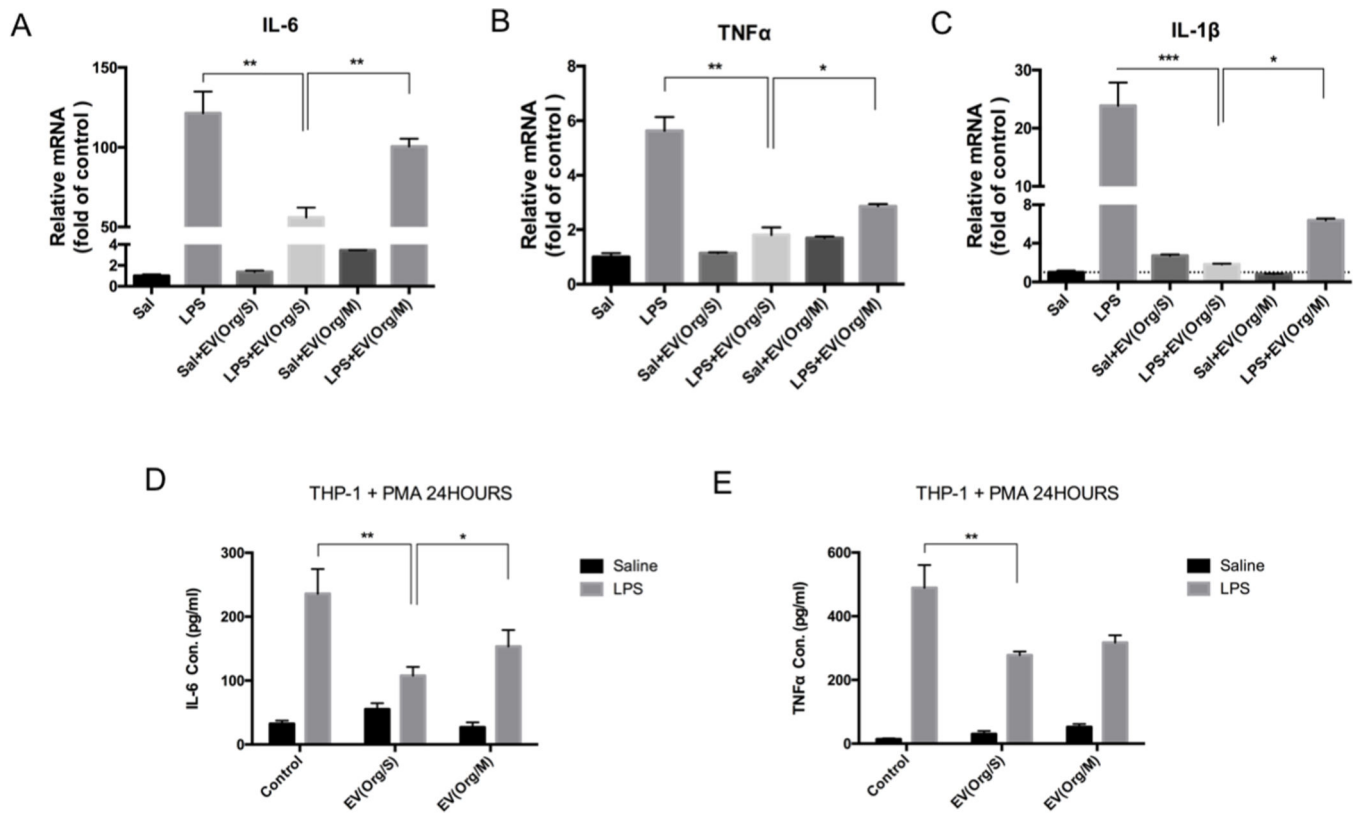


Figure 3. EVs derived from human colonic organoid modulated immune responses of human macrophages to endotoxin stimulation.

Human monocyte THP-1 were first differentiated to macrophages with PMA treatment for 24 hours, after which these macrophages were incubated with EV(Org/S) or EV(Org/M) and then stimulated with LPS for 4 hours. Total RNA of differentiated THP-1 was extracted for qPCR and the supernatant was collected for ELISA. qPCR analysis of IL-6 (A), TNFα (B) and IL-1β (C). ELISA analysis of IL-6 (D) and TNFα (E). (sal: saline; LPS: Lipopolysaccharide; EV(Org/S): EVs purified from the supernatant of organoid culture pretreated with saline; EV(Org/M): EVs purified from the supernatant of organoid culture pretreated with morphine. The results are expressed as the mean ± SEM of triplicate measurements in each group, *p<0.05, **p<0.01, ***p<0.001).

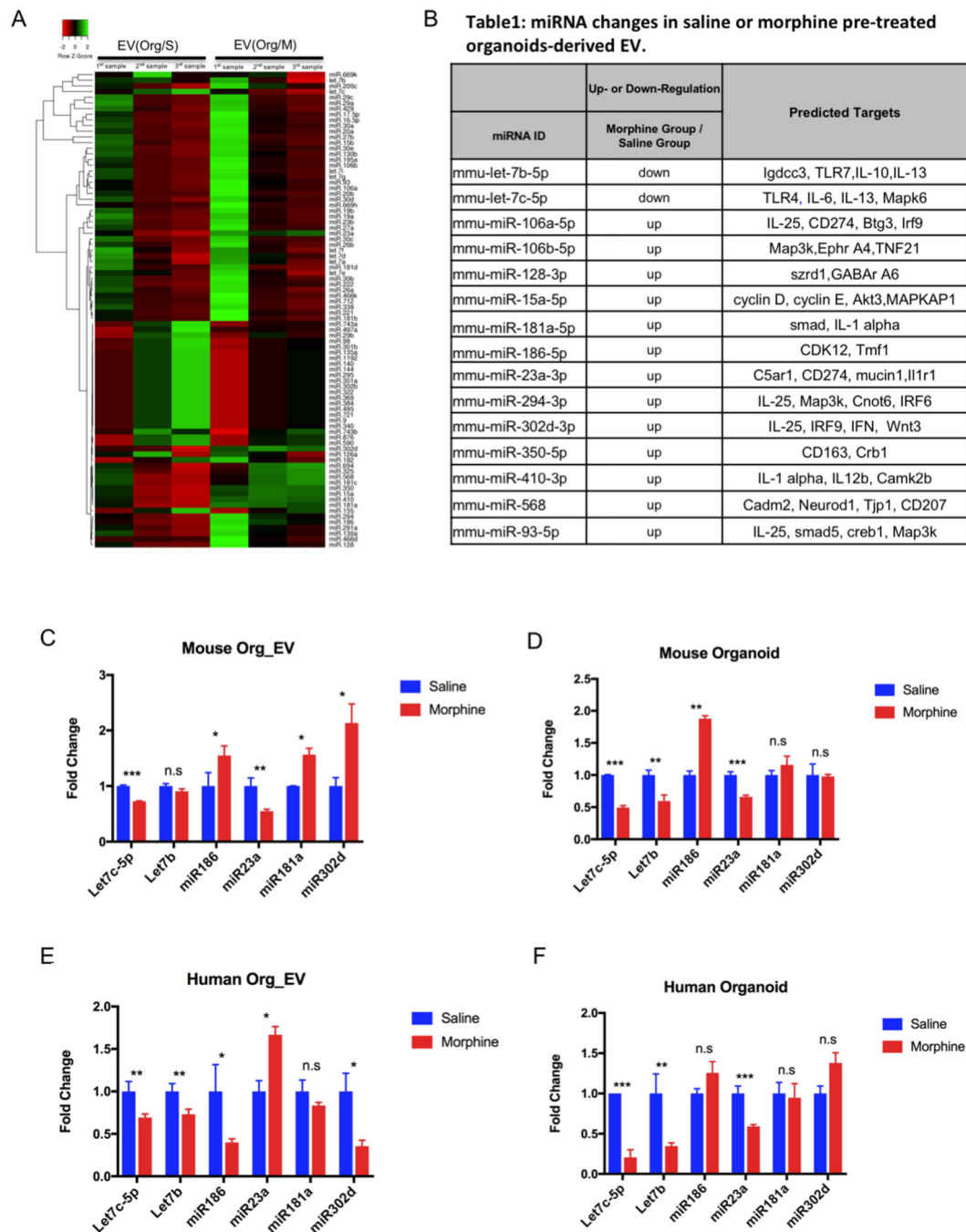


Figure 4. The microRNA profile in organoid-derived EVs and organoids.

(A) Heat map of microRNA microarray expression in EV samples derived from mouse small intestinal organoid that were pre-treated with saline (EV(Org/S)) (n=6) or morphine (EV(Org/M)) (n=6). (B) Various inflammation related genes were predicted with Target-Scan database (<http://www.targetscan.org>) to be the targets of the microRNAs whose levels were changed in the EV samples shown in (A). (C) The change of individual microRNA levels in EV samples derived from mouse small intestinal organoids that were treated with saline or morphine. (D) The change of individual microRNA levels in the mouse small

intestinal organoids that were treated with saline or morphine. (E) The change of individual microRNA levels in EV samples derived from human colonic organoid that were treated with saline or morphine. (F) The change of individual microRNA levels in human colonic organoids that were treated with saline or morphine. The results are expressed as the mean \pm SEM of triplicate measurements in each group, * $p < 0.05$, ** $p < 0.01$, *** $p < 0.001$).

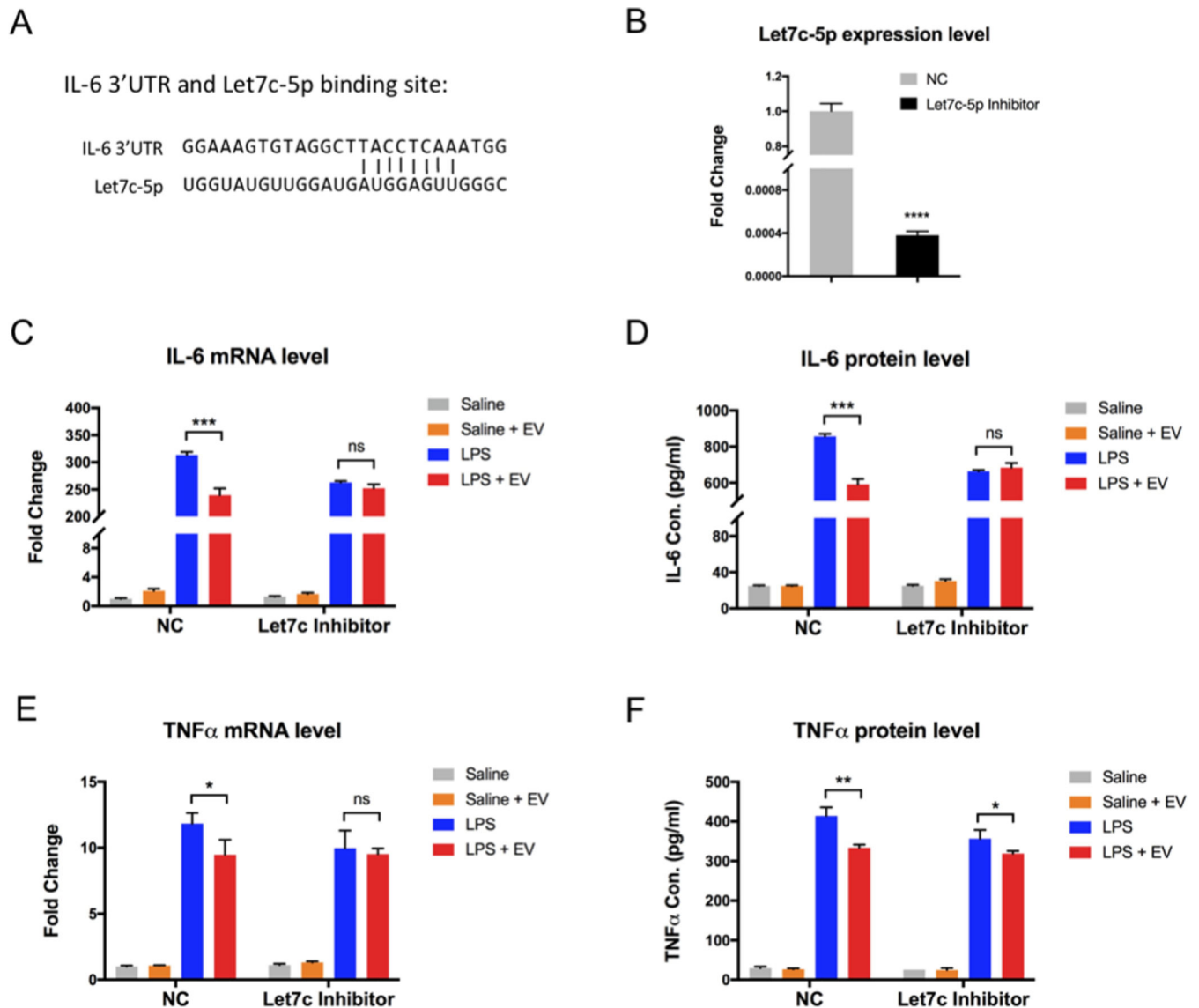


Figure 5. The effect of EVs on inflammatory cytokine expression was mediated by Let7c-5p. (A) The binding site of Let7c-5p on IL-6 mRNA 3'-UnTranslated Region (3'-UTR). (B) Let7c-5p level was decreased when BMDC were transfected with the LNA microRNA inhibitor for Let7c-5p. 72Hrs post-transfection, the microRNA from BMDC was extracted to check Let7c-5p level. (C, E) 72Hrs after transfection of Negative control inhibitor (NC) or Let7c-5p inhibitor, BMDC were treated with LPS alone or together with the EVs that were derived from mouse small intestinal organoid. 4Hrs later total RNA from BMDC was extracted to check IL-6(C) and TNF α (E) mRNA levels. (D, F) The supernatants of BMDC were collected to measure the IL-6 (D) and TNF α (F) levels through ELISA. The results are expressed as the mean \pm SEM of triplicate measurements in each group, * p <0.05, ** p <0.01, *** p <0.001).

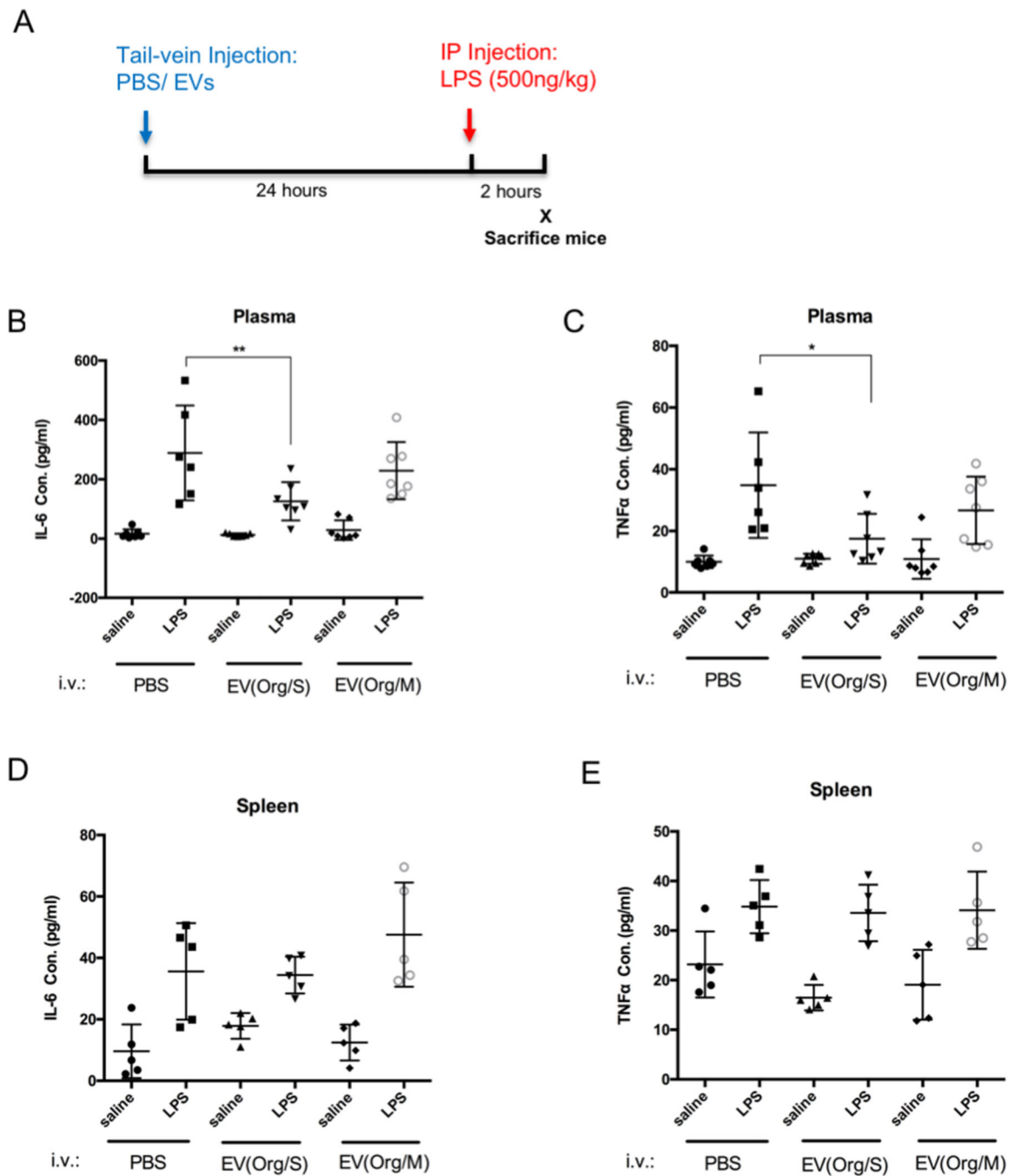


Figure 6. Intravenous injection of EVs from saline-treated intestinal organoids reduced the LPS-induced systemic inflammation in mice, while EVs from morphine-treated organoids did not have such effect.

(A) Experiment timeline. (B-E) Measurement of pro-inflammatory cytokines IL-6 and TNF α in the plasma (B-C) and spleen (D-E) by ELISA. (The results are expressed as the mean \pm SEM of measurements from N=5–12 per group, and each dot represents a measurement from one animal; * p <0.05, ** p <0.01).

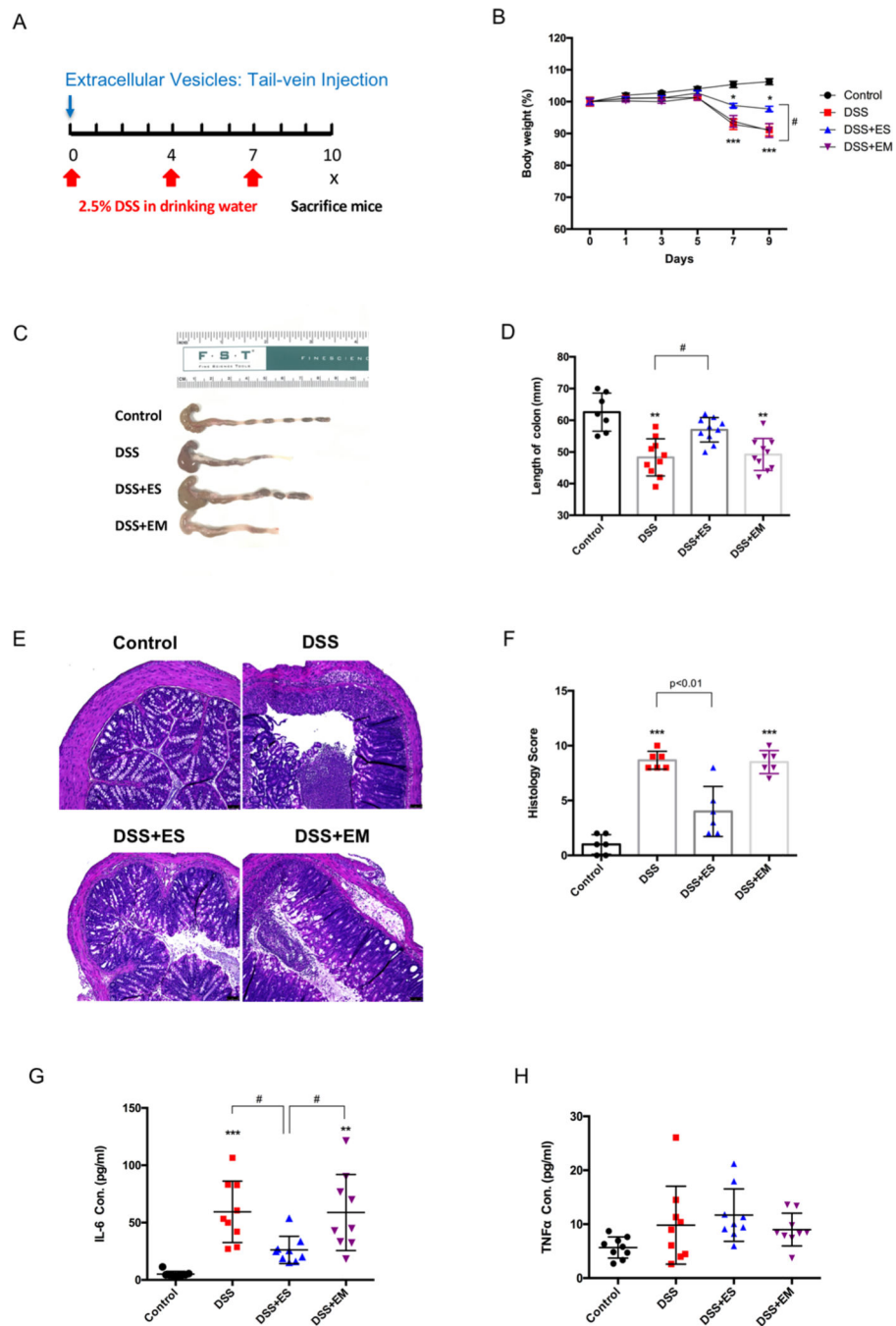


Figure 7. Intravenous injection of EVs from saline-treated intestinal organoid (ES) alleviated DSS-induced colitis symptoms in mice, while EVs from morphine-treated organoids (EM) did not show these effects.

(A) Experiment timeline. (B) Measurements of mice body weight in each group. (C-D) The length of colon in each group showed significant difference by EVs i.v. injection. (E) Representative images of colon tissue with H&E staining of control and DSS treated mice (Scale bars, 50 μ m). (F) The histology scores were estimated according to the scoring system for colitis. (G-H) Measurement of pro-inflammatory cytokines IL-6 and TNF α in the plasma of each group of mice by ELISA. (The results are expressed as the mean \pm SEM of

measurements from N=6–10 animals per group, and each dot represents a measurement from one animal; *p<0.05, **p<0.01, ***p<0.001).

Author Manuscript

Author Manuscript

Author Manuscript

Author Manuscript

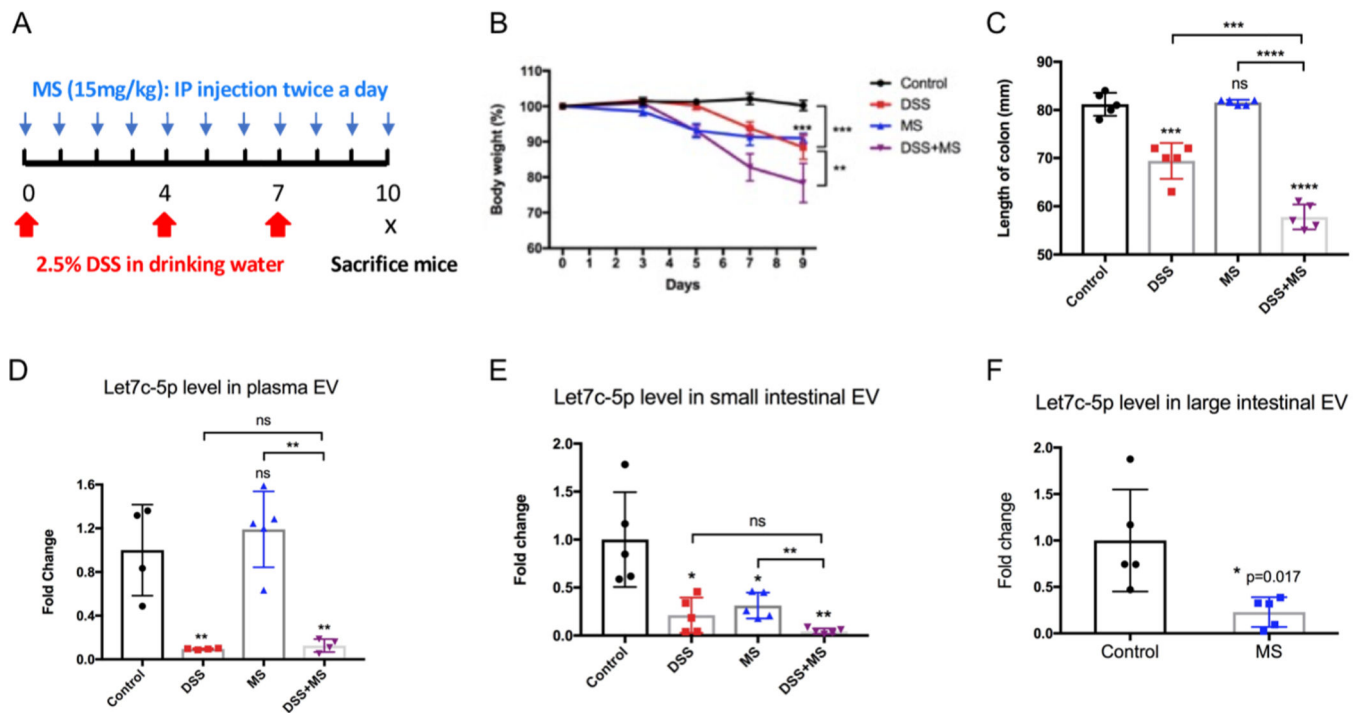


Figure 8. Let7c-5p levels in EVs isolated from plasma, small intestine and large intestine were reduced in DSS/Morphine treated mice.

(A) Experiment design and timeline. On day 0, 2.5% DSS was added in drinking water which was replaced with fresh 2.5% DSS drinking water on day4 and day7. Morphine sulfate (15mg/kg) was injected through IP twice a day until day10 when the mice were sacrificed. For each experiment group n=5. (B) Mice body weight change in each group. (C) The length of colon showed a significant difference. (D- F) Let7c-5p levels in EVs that were isolated from the plasma (D), small intestine (E) and large intestine (F) were measured through real-time PCR. U6 was used as internal control. (The results are expressed as the mean \pm SEM of measurements from N=4–5 animals per group, and each dot represents a measurement from one animal; *p<0.05, **p<0.01, ***p<0.001).

Table 1.

Primary antibodies used in western blot assay.

	Species	Dilution	Cat.#	Brand
CD63 (H-193)	Rabbit	1:200	SC-15363	Santa Cruz (Dallas, TX, US)
CD 9 (EM-04)	Rat	1:500	MA1-10309	Thermo Fisher Scientific (Waltham, MA, US)
Tsg101	Rabbit	1:1000	ab30871	Abcam (Cambridge, UK)
β Actin	Mouse	1:4000	4967S	Cell Signaling Technology (Danvers, MA,US)
GAPDH	Rabbit	1:2000	PA1-987	Thermo Fisher Scientific (Waltham, MA, US)

* Abbreviations:

Tsg101: Tumor susceptibility gene 101 protein

GAPDH: Glyceraldehyde 3-phosphate dehydrogenase

Table 2.

Primer used in real-time PCR assay.

IL-6 F	mouse	CCGGAGAGGAGACTTCACAG
IL-6 R	mouse	TCCACGATTCCCAGAGAAC
IL-1 β F	mouse	GGCAGGCAGTATCACTCATT
IL-1 β R	mouse	AAGGTGCTCATGTCCTCATC
TNF α F	mouse	GACGTGGAACGGCAGAAGA
TNF α R	mouse	GCCACAAGCAGGAAT GAGAA
IL-4 F	mouse	AGATCATCGGCATTTTGAACG
IL-4 R	mouse	TTTGGCACATCCATCTCCG
IL-25 F	mouse	CGGAGGAGTGGCTGAAGTGGAG
IL-25 R	mouse	ATGGGTACCTTCCTCGCCATG
IL-10 F	mouse	CGGGAAGACAATAACTGCACCC
IL-10 R	mouse	CGGTTAGCAGTATGTTGTCCAGC
TGF β F	mouse	CCTGTCCAAACTAAGGC
TGF β R	mouse	GGTTTTCTCATAGATGGCG
rpL32A F	mouse	GCTGGAGGTGCTGCTGATGT
rpL32A R	mouse	ACTCTGATGGCCAGCTGTGC
IL-6 F	Human	AACCTGAACCTTCCAAAGATGG
IL-6 R	Human	TCTGGCTTGTTCCCTCACTACT
IL-1 β F	Human	CAGCTACGAATCTCCGACCAC
IL-1 β R	Human	GGCAGGGAACCAGCATCTTC
TNF α F	Human	ATGAGCACTGAAAGCATGATCC
TNF α R	Human	GAGGGCTGATTAGAGAGAGGGTC
TGF β F	Human	TACCTGAACCCGTGTGCTCTC
TGF β R	Human	GTTGCTGAGGTATCGCCAGGAA
IL-4 F	Human	CCAACTGCTTCCCCCTCTG
IL-4 R	Human	TCTGTTACGGTCAACTCGGTG
IL-10 F	Human	TCAAGGCGCATGTGAACTCC
IL-10 R	Human	GATGTCAAACCTCACTCATGGCT
β actin F	Human	TCCTCTCCAAGTCCACACAGG
β actin R	Human	GGGCACGAAGGCTCATCATT